Sodium-23 and potassium-39 nuclear magnetic resonance relaxation in eye lens. Examples of quadrupole ion magnetic relaxation in a crowded protein environment

Arthur Stevens, Peter Paschalis, and Thomas Schleich
Department of Chemistry and Biochemistry, Sinsheimer Laboratories, University of California, Santa Cruz, California 95064

ABSTRACT Single and multiple quantum nuclear magnetic resonance (NMR) spectroscopic techniques were used to investigate the motional dynamics of sodium and potassium ions in concentrated protein solution, represented in this study by cortical and nuclear bovine lens tissue homogenates. Both ions displayed homogeneous biexponential magnetic relaxation behavior. Furthermore, the NMR relaxation behavior of these ions in lens homogenates was consistent either with a model that assumed the occurrence of two predominant ionic populations, "free" and "bound," in fast exchange with each other or with a model that assumed an asymmetric Gaussian distribution of correlation times. Regardless of the model employed, both ions were found to occur in a predominantly "free" or "unbound" rapidly reorienting state. The fraction of "bound" $^{23}Na^+$, assuming a discrete two-site model, was ~0.006 and 0.017 for cortical and nuclear homogenates, respectively. Corresponding values for $^{39}K^+$ were 0.003 and 0.007, respectively. Estimated values for the fraction of "bound" $^{23}Na^+$ or $^{39}K^+$ obtained from the distribution model ($\tau_c > \omega_L^{-1}$) were ≤ 0.05 for all cases examined. The correlation times of the "bound" ions, derived using either a two-site or distribution model, yielded values that were at least one order of magnitude smaller than the reorientational motion of the constituent lens proteins. This observation implies that the apparent correlation time for ion binding is dominated by processes other than protein reorientational motion, most likely fast exchange between "free" and "bound" environments. The results of NMR visibility studies were consistent with the above findings, in agreement with other studies performed by non-NMR methods. These studies, in combination with those presented in the literature, suggest that the most likely role for sodium and potassium ions in the lens appears to be the regulation of cell volume by affecting the intralenticular water chemical potential.

INTRODUCTION

The vertebrate eye lens represents an excellent system for the study of biophysical phenomena of relevance to biomedical applications. In part this is because the mature lens fiber cells contain an unusually high protein content, consisting primarily of a group of three stable proteins collectively referred to as the crystallins (1). Crystallin protein concentrations of ~250 and 400 mg/mL characterize the cortical (outer) and nuclear (inner) lens regions, resulting in a gradient with a high protein packing density. Furthermore, the extracellular space of the lens is small.

The relative simplicity of lens fiber cell cytoplasm facilitates study of lens constituents, such as quadrupolar ion ($I \geq 1$) magnetic resonance behavior. For lens tissue, the maintenance of normal function in part depends on the behavior of constituent sodium and potassium ions, i.e., on their intralenticular state (2). Insights into the intracellular state of these ions is afforded by a determination of their quadrupolar ion NMR relaxation characteristics, which in single and multiple quantum experiments is critically dependent on both the ionic motional timescale and the degree of surrounding microscopic order (3) and thus is a reflection of the immediate molecular environment of the ion.

Of the two ions, $^{23}Na^+$ has been the most extensively studied, primarily because of its natural high abundance, its relatively large gyromagnetic ratio, and its short nuclear magnetic relaxation times. The magnetic relaxation behavior of $^{23}Na^+$ in a variety of biological systems has been studied in detail (for reviews see reference 4–6). By contrast, $^{39}K^+$ has been less extensively studied even though its intracellular concentration is at least five times greater than that of $^{23}Na^+$. This is reflected in the literature, where the majority of the research on the behavior of quadrupolar ionic nuclei has focussed on $^{23}Na^+$ (6–9). However, with advances in NMR instrumentation the low sensitivity of $^{39}K^+$ has become less of a problem, and recently, several papers have appeared describing the results of double quantum filtered $^{39}K^+$ NMR experiments involving tissue systems (10–12). The low sensitivity of $^{39}K^+$ may be ameliorated in certain instances by the addition of exogenous ion or be circumvented by using $^{87}Rb^+$, a biological congener of $^{39}K^+$, which enjoys higher sensitivity, in NMR experiments (13, 14).

Previous studies on these ions in lens tissue have primarily been aimed on their distribution (15) and have shown that K^+ is actively transported into the lens at the epithelium with diffusion proceeding posteriorly, thereby generating a concentration gradient. By contrast, Na^+

0006-3495/92/05/1061/15 $2.00

enters the lens across the posterior capsule and diffuses anteriorly to be actively extruded by the lens epithelium. In both cases a Na/K-ATPase driven pump–leak system has been proposed to explain the ion gradient formed across the lens and the concentration differences between the lens and the aqueous and vitreous humors (16–18).

Several quadrupolar ion NMR studies performed on lens tissue have used $^{23}Na^+$. One study (19) demonstrated that the $^{23}Na^+$ transverse relaxation time (28 ms) was shorter than the longitudinal relaxation time (38 ms) at 4.7 T, indicating that a fraction of the intralenticular $^{23}Na^+$ occurred in the nonextreme narrowing motional timescale, i.e., in a mode of reduced or restricted motion, possibly the result of ion binding to lens proteins. By contrast, $^{23}Na^+$ magnetic resonance imaging conducted at 2.7 T of the bovine lens (20) indicated the presence of two major T_2 components, one fast (3 ms) and the other slow (28 ms). Furthermore, the Na^+ concentration gradient visualized by the lens imaging experiment was consistent with that predicted by the pump–leak model.

Non-NMR studies have revealed that a fraction of nonexchangeable (nondiffusible) Na^+ occurs in lens tissue (21). Sodium ion populations of restricted mobility have also been detected in other biological systems, such as aqueous solutions of bovine serum albumin (3), rat muscle (22), and plasma (23).

Of the magnetic resonance studies performed on $^{39}K^+$, essentially similar findings were obtained to those of $^{23}Na^+$ (6). Relaxation rate constants for $^{39}K^+$ in tissue are typically two to three times greater than those obtained for $^{23}Na^+$ (6). Few studies have simultaneously examined, in detail, the properties of $^{23}Na^+$ and $^{39}K^+$ in the same tissue (12).

The purpose of this study was to investigate the motional dynamics of $^{23}Na^+$ and $^{39}K^+$ in bovine cortical and nuclear lens tissue by the use of single and multiple quantum NMR techniques, as a means of characterizing the intralenticular state of these ions. NMR visibility studies were also performed to examine whether any fraction of $^{23}Na^+$ or $^{39}K^+$ ions were immobilized, and thus, invisible to the NMR techniques usually employed.

THEORETICAL BACKGROUND

Isolated spin ½ quadrupolar nuclei, such as ^{23}Na and ^{39}K, have four Zeeman energy levels, which under appropriate environmental conditions and excitation regimes can sustain single, double, or triple quantum NMR transitions (24–28) The central or "inner" transition ($m = -½ \rightarrow +½$) is flanked by a pair of satellite or "outer" transitions ($m = ³/₂ \rightarrow ½$; $m = -½ \rightarrow -³/₂$). The NMR spectral characteristics of spin ³/₂ nuclei are established by the relationship of the correlation time (τ_c) for molecular fluctuations in the ionic hydration shell to ω_L^{-1} and $\bar{\omega}_Q^{-1}$, where ω_L is the angular Larmor precessional frequency and $\bar{\omega}_Q$ is the time-averaged value of the frequency of the satellite transition relative to ω_L. In the absence of long range order, the effective value of $\bar{\omega}_Q$ is zero when averaged over a time. If $\tau_c \ll \bar{\omega}_L^{-1}$, i.e., the extreme motionally narrowed condition, all transitions occur at the same frequency and are characterized by identical longitudinal (T_1) and transverse (T_2) relaxation times. Multiple quantum excitation is forbidden in this circumstance (3, 28). However, if $\omega_L^{-1} \leq \tau_c \leq \bar{\omega}_Q^{-1}$, the three degenerate single quantum transitions are characterized by biexponential longitudinal and transverse relaxation (3, 28), i.e., the nonextreme motionally narrowed situation.

For most biological samples, homogeneous biexponential (type *c* [3]) spectra have been observed. In this case the longitudinal magnetization is given by

$$M_o - M_z(t) = M_o[0.8 \exp(-R_{1S}t) + 0.2 \exp(-R_{1F}t)], \quad (1)$$

where R_{1S} and R_{1F} are the relaxation rate constants for the slow and fast transitions decay of the longitudinal magnetization; the other symbols have their usual meaning (29). Inversion recovery experiments performed on quadrupolar ionic nuclei usually fail to clearly reveal the biexponential nature of the recovering longitudinal magnetization, yielding an observed rate constant R_{1lin} whose value lies between R_{1S} and R_{1F}.

The corresponding expression for relaxation behavior of the transverse magnetization is described by

$$M_x(t) = M_o[0.4 \exp(-R_{2S}t) + 0.6 \exp(-R_{2F}t)], \quad (2)$$

where R_{2S} and R_{2F} are the relaxation rate constants representing the slow and fast transitions decay of the transverse magnetization (29).

For ionic populations characterized by a single correlation time and for which $\bar{\omega}_Q = 0$, the expressions for R_{1S}, R_{1F}, R_{2S}, R_{2F}, and R^{2Q} are given by Eq. 3 (28, 29, 30):

$$R_{1S} = 0.4\pi^2\chi^2 J_2(2\omega_L) \quad (3a)$$

$$R_{1F} = 0.4\pi^2\chi^2 J_1(\omega_L) \quad (3b)$$

$$R_{1lin} = 0.4\pi^2\chi^2[0.2J_1(\omega_L) + 0.8J_2(2\omega_L)] \quad (3c)$$

$$R_{2S} = 0.2\pi^2\chi^2[J_1(\omega_L) + J_2(2\omega_L)] \quad (3d)$$

$$R_{2F} = 0.2\pi^2\chi^2[J_0(0) + J_1(\omega_L)] \quad (3e)$$

$$R^{2Q} = 0.2\pi^2\chi^2[J_0(0) + J_2(2\omega_L)], \quad (3f)$$

where $\chi = e^2qQ/h$ is the quadrupole coupling constant in Hz, R^{2Q} is the rate constant for the decay of the double quantum transitions, and $J_n(n\omega_L)$ is the spectral

density function, which is given by

$$J_n(n\omega_L) = \frac{\tau_c}{1 + n^2(\omega_L\tau_c)^2}. \quad (4)$$

τ_c is the correlation time for exponential decay of the molecular fluctuations in the electric field gradient (EFG) tensor responsible for relaxation. For simplicity, the asymmetry parameter (28) is set to zero and a single (average) correlation time is assumed to characterize the molecular fluctuations in a particular state, e.g., "free" or "bound." The latter simplification does not take into account the likely occurrence of microenvironments, which would lead to a distribution of correlation times (31) and is considered below.

For a homogeneous biexponential (type *c*) spin 3/2 quadrupolar nucleus, the time dependent signal after double quantum filtration is given by

$$S_{2Q}(t_2) = 0.15\,[M_o f(\tau) f(t_2) \times \exp(-R^{2Q}t_1)\cos(2\delta t_1)\exp(i\delta t_2)], \quad (5)$$

where $f(\tau) = \exp(-R_{2S}\tau) - \exp(-R_{2F}\tau)$, $f(t_2) = \exp(-R_{2S}t_2) - \exp(-R_{2F}t_2)$, δ is the resonance offset, τ is the preparation time, and t_1 is the evolution time for the generation of multiple quantum coherence; the other symbols have their usual meaning. The optimum value of τ is given by

$$\tau_{opt} = \frac{1}{R_{2S}}\frac{\ln(\alpha)}{(\alpha - 1)}, \quad (6)$$

where $\alpha = R_{2F}/R_{2S}$ (28).

Incrementation of t_1 leads to a two-dimensional data set which upon Fourier transformation, results in a two-dimensional spectrum. R^{2Q} values can be obtained from the linewidth of the ν_1 projection of a full two-dimensional experiment or, preferably, from a less time consuming pseudo two-dimensional experiment using selected t_1 values for incrementation.

At constant t_1, variation of τ gives double quantum filtered signals of relative amplitude,

$$S_{rel} = \frac{S(\tau)}{S(\tau_{ref})} = \frac{f(\tau)}{\exp(-R_{2S}\tau_{ref}) - \exp(-R_{2F}\tau_{ref})}, \quad (7)$$

from which R_{2S} and R_{2F} can be obtained. Analogously, double quantum filtration experiments performed at constant τ but with variable t_1 permits the evaluation of R^{2Q} from the expression

$$\ln(S_{rel}) = \ln\left(\frac{S(t_1)}{S(t_{1,ref})}\right) = -R^{2Q}(t_1 - t_{1,ref}) \quad (8)$$

Biological systems, because of their inherent complexity, are expected to contain a heterogeneous population of ionic nuclei, where each individual population state is characterized by a particular value of the quadrupolar coupling constant, the correlation time for fluctuations of the EFG tensor, and the ionic mean lifetime (τ_{ex}). To evaluate the ionic correlation times in lens tissue two different models were employed. The first model assumed only two ionic states, "free" and "bound," in fast exchange on the relaxation time timescale. In this context, a lengthening of the correlation time, implying more restricted motion, was assumed to represent the "bound" state.

Under the condition of fast exchange between two discrete populations, A and B, the observed longitudinal and transverse relaxation rate constants are expressed as a sum of the respective rate constants, each weighted by its respective mole fraction, Θ_A and Θ_B. Thus,

$$R_X = \Theta_A(R_X)_A + \Theta_B(R_X)_B, \quad (9)$$

where R_X represents any of the individual relaxation rate constants that appear in Eq. 3. If A represents the population of "free" ions, and $\omega\tau_c \ll 1$, then each of the individual $(R_X)_A$ terms are equal to each other and may simply be referred to as R_A. Furthermore, the overall correlation time of the bound state, $\tau_{c,B}$, which represents binding of the ion to macromolecular species, may include contributions from the lifetime of the bound nuclear spin (τ_{ex}), if τ_{ex} is approximately equal to or less than τ_c (32).

Recently, it has been suggested by Rooney and Springer (33, 34) that it may be more realistic to represent the correlation times of a population of ions in tissue in terms of a distribution (35, 36). The approach used here follows that employed by Rooney and Springer (33, 34), which was originally adopted by Merbolt and Frahm (37) to adequately represent the water proton relaxation behavior of binary and ternary mixtures. The average value of the relaxation rate constant for the population is defined as follows:

$$\overline{R}_X = \int_0^\infty p(\tau_c)R_X(\tau_c)\,d\ln(\tau_c), \quad (10)$$

where $p(\tau_c)$ is the distribution function for the correlation time and is represented by an asymmetric Gaussian function of the form

$$p(\tau_c) = N\exp\left(-a^2\left(\ln\frac{\tau_c}{\tau_m}\right)\right)^2 \quad (11a)$$

$$p(\tau_c) = N\exp\left(-b^2\left(\ln\frac{\tau_c}{\tau_m}\right)\right)^2, \quad (11b)$$

where Eq. 11*a* and 11*b* apply when $\tau_c \leq \tau_m$ and $\tau_c > \tau_m$, respectively. The term τ_m represents the modal value of the distribution of correlation times. The constants *a*

and b represent the half-widths of the distribution and N represents the normalization factor, which is given by

$$N = \frac{2ab}{a+b}. \quad (12)$$

In the analysis of the distribution of the correlation times, the lower limit of the correlation time was arbitrarily set to 10^{-15} s, whereas the upper limit was placed, because of limitations in the applicability of type c relaxation equations (derived using second-order perturbation theory), at 10^{-6} s ($\kappa = (\chi/\omega_L)^2 6\omega_L\tau_c \leq 1$) (38).

EXPERIMENTAL PROCEDURES

Lens homogenate preparation

Calf lenses (1 day to 3 mo old calves) were obtained from a local abattoir and kept on ice until the lenses were removed (typically within a few hours of slaughter) to avoid uptake or release of ions into the aqueous and/or vitreous humor. Cortical and nuclear lens homogenates were prepared as previously described (39). In some experiments the concentration of $^{39}K^+$ in lens homogenates was increased to 450 mM by the addition of solid KCl.

NMR measurements and data analysis

Experiments were performed using a General Electric (GE) GN-300 spectrometer (General Electric Co., Wilmington, MA) equipped with an Oxford Instruments (Columbia, MD) 7.05 T wide-bore (89 mm) magnet. A GE 12-mm broadband probe was used for $^{23}Na^+$ whereas for $^{39}K^+$ a 12-mm fixed-frequency GE probe was used. In both cases 12-mm (o.d.) NMR tubes (nonspinning) were used for all measurements. In addition, some $^{23}Na^+$ NMR measurements were made using a GE GN-500 spectrometer (General Electric Co.). Sample temperature was regulated to within ±0.5°C of the desired value.

Five different types of experiments were performed to characterize the relaxation parameters of the ions: 90° one-pulse (1PULS), T_1 inversion recovery (T1IR), one-dimensional double quantum filtration with τ (preparation time) incrementation at constant t_1 (double quantum evolution time) (1DDQ), two-dimensional double quantum with t_1 incrementation (2DDQ) at constant τ, and pseudo 2DDQ with selected t_1 incrementation (at constant τ). The later three experiments were carried out using the double quantum excitation (filter) pulse sequence: $[(\pi/2)_x - \tau/2 - (\pi)_y - \tau/2 - (\pi/2)_x - t_1 - (\pi/2)_x - \text{acquire } (t_2)]$ (40–42). A 32-step phase cycle sequence (41) was used to suppress unwanted signals and coherent noise. The spectral width and digital resolution in the ν_1 dimension as well as the preparation time (τ) were optimized for each sample as described previously (3).

Typical parameters employed for spectral acquisition were as follows: (1PULS) 90° tipping pulse, 41.5 ($^{23}Na^+$), 51.0 ($^{39}K^+$) μs; sweep width, ±5,000 Hz (quadrature phase detection); acquisition delay, 75–300 μs; 1,024 data points. For 1PULS and T1IR experiments, the repetition time was approximately equal to the acquisition time ($\sim 5\,T_{1lin}$), whereas in double quantum filtered sequences the repetition time was 9–10 T_{1lin}. If the repetition time was shorter than this value, unwanted signal, which was stronger at smaller τ values, passed through the filter. This phenomenon, which has been observed in other studies (7), most likely arises from incomplete cancellation of large single quantum spectral components that remain at repetition times of $\sim 5T_{1lin}$, and thus longer times are required. The remaining parameters of each pulse sequence are tabulated in Table 1. All experiments were performed on-resonance, i.e., with a zero offset excitation ($\Delta\nu_{off} \leq 10$ Hz).

Spectral data processing was performed on a Nicolet

TABLE 1 Instrument parameters employed for the measurement of $^{23}Na^+$ and $^{39}K^+$ magnetic resonance parameters

NMR experiment	$^{23}Na^+$	$^{39}K^+$
One pulse		
Acquisition delay (μs)	70–200	75–300
Number of accumulations	≤8,000	64,000
T1IR		
Acquisition delay (μs)	75–150	75–300
Number of τ values	11–15	11–15
Number of accumulations per τ value	200	10,000–20,000
1DDQ		
Acquisition delay (μs)	20–30	30–50
t_1 (μs)	10	10
Number of τ values (0–3 T_{1lin})	15–20	15–20
Number of accumulations at each τ value (integral number of 32)	10,000–20,000	≤96,000
Repetition time	≥9–10 T_{1lin}	≥9–10 T_{1lin}
2DDQ*		
Acquisition delay (μs)	20–30	30–50
τ	τ_{opt}	τ_{opt}
Number of accumulations per τ value	4800–9120	≥96,000
t_1 (μs)	40–80	10

*For $^{39}K^+$ only pseudo 2DDQ data were taken.

1280 data station using GEN software (version 8) for both one- and two-dimensional NMR experiments. Absolute value spectra were calculated for the two-dimensional NMR experiments. NMR data reduction was also performed by the use of other software on either an IBM PS/2 Model 70 computer (IBM Instruments Inc., Danbury, CT) or SUN Sparc 1+ workstation. The number of time-dependent components present in an exponentially varying data set was independently evaluated using a Hankel singular value decomposition (HSVD) algorithm (43–45) written using either the 386-MATLAB® or SUN PRO-MATLAB® software packages (The Mathworks, Inc., South Natick, MA). The HSVD routine provides a plot of the singular values as a function of array index from which the number of time-dependent components was determined. In addition, the amplitude, time constant, and phase of each component were also obtained. Non-linear regression analyses were performed using the NONLINWOOD routine (46) or the Marquardt-Levenberg algorithm contained in the SIGMAPLOT® (version 4.0) software package (Jandel Sci., Corte Madera, CA).

NMR visibility studies

Cortical and nuclear homogenates were weighed (~2.0 g) and 10 mL of either distilled water or concentrated HNO_3 was added. The mixtures were incubated at 50°C for 3 days and weighed again to ensure that the concentration was unaltered before spectral analysis. The samples were then appropriately diluted for atomic absorption or measured using single pulse NMR experiments.

The concentration of Na^+ and K^+ was determined at 589 nm and 766.5 nm, respectively, using an atomic absorption spectrometer (model 2380; Perkin Elmer Corp., Norwalk, CT). At these wavelengths, signal intensity is linearly proportional to concentration in the range between 0 and 2 ppm. All measurements were performed in duplicate. The reproducibility of the measurements was 5% for Na^+ and 10% for K^+.

Quadrupolar ion NMR visibility was assessed by comparing the peak area of the tissue signal with the quadrupolar ion resonance signal intensity obtained from $^{23}Na^+$ or $^{39}K^+$ in water and concentrated HNO_3 at a known concentration. The experimental NMR parameters used for the measurements are given in Table 1. The data obtained were corrected for signal loss occurring during the receiver dead time by employing an exponentially weighted sum (0.4:0.6) of the relaxation rate constants R_{2S} and R_{2F}. Typical correction factors used were 0.5–11.0% for $^{23}Na^+$ and 2.5–26.5% for $^{39}K^+$.

Simulations

Spectral simulations were performed using routines written in Borland Turbo Pascal (version 5.0). The MATLAB® software package was also employed. Copies of the software routines are available upon request, preferably by E-mail to: yoti@aku.ucsc.edu.

RESULTS

Simulation studies

Single and double quantum filtered $^{23}Na^+$ spectra were simulated (by Fourier transformation of Eqs. 2 and 5, respectively) as a function of correlation time in the range $2.0 \times 10^{-9} \leq \tau_c \leq 1.0 \times 10^{-7}$ s ($\kappa = 0.14$). The relevant relaxation rate constants defining the spectral lineshapes are described by Eqs. 3 and 4. In each case, the nonLorentzian lineshape character of the single quantum $^{23}Na^+$ was evident (spectra not shown), although with increasing τ_c the contribution from the rapidly relaxing transitions was broadened significantly, resulting in an apparent loss of the broad component. This phenomenon was also largely responsible for the double quantum filtered lineshape changes shown in Fig. 1. In this case, the spectral contributions to the total lineshape are in antiphase, resulting in a disappearance of the characteristic "double hump" spectral lineshape signature of a double quantum filtered spectrum with increasing correlation time.

A discrete two-site fast exchange ($1/\tau_{ex} \gg R_{2F}$) model to mimic exchange between an "unbound" $^{23}Na^+$ population in excess with a minor "bound" population, as might occur in tissue, was also simulated. In this case, the overall relaxation rate constant is dependent on the mole fraction weighting of the "free" and "bound" relaxation rate constants (see Eq. 9). Correlation times of 0.01 and 10 ns were assumed for the "free" and "bound" Na^+, respectively, and Θ_B values of 0.001, 0.01, and 0.1 were used. The calculated double quantum filtered spectra are shown in Fig. 2. "Double hump" spectral lineshape signatures were observed at very small bound mole fraction values (e.g., 0.001). With increasing Θ_B the double quantum filtered spectral lineshape broadens significantly, resulting in an apparent loss of the broad component.

Experimental studies

Fig. 3*A* and *B* show typical $^{39}K^+$ absorption spectra obtained from calf cortical and nuclear homogenates, respectively, containing physiological normal concentrations of K^+. The $^{39}K^+$ spectra shown in Fig. 3 were

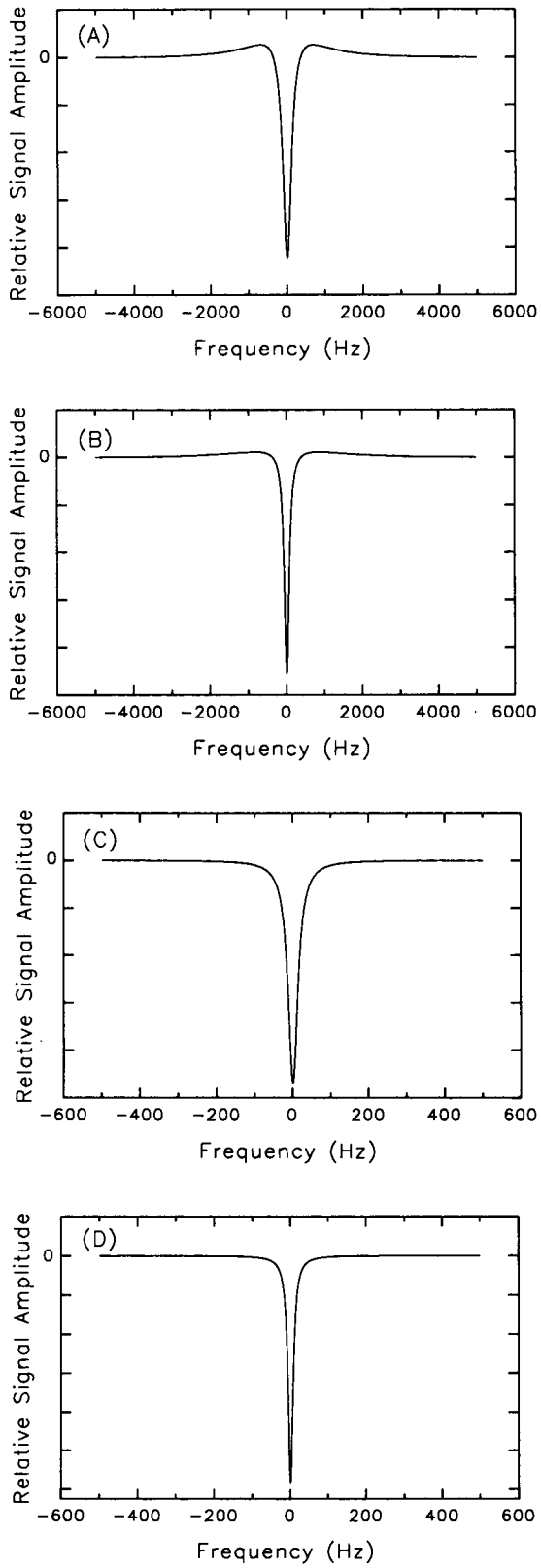

simulated by the summation of two in-phase Lorentzian lineshapes differing in width. For cortical homogenate, the narrow component (line width at half-height = 42 Hz) accounted for 40.0% of the total $^{39}K^+$ signal intensity, whereas the broad resonance component (line width = 128 Hz) constituted the remainder. Corresponding values for nuclear homogenate were narrow component, 40.1% of the total $^{39}K^+$ signal intensity (line width = 78 Hz), and broad component, 59.9% of the total (line width = 306 Hz). Similar spectra were obtained for $^{23}Na^+$ (not shown). For cortical homogenate, the $^{23}Na^+$ narrow component (line width at half-height = 30 Hz) contributed 41.0% of the total $^{23}Na^+$ signal intensity; the broad resonance component contributed 59.0% of the total (line width = 288 Hz). Corresponding $^{23}Na^+$ values for nuclear homogenate were narrow component, 39.0% of the total $^{23}Na^+$ signal intensity (line width = 55 Hz), and broad component, 61.0% of the total (line width = 612 Hz). The relative signal intensities for the narrow and broad spectral components conform to theoretical expectations.

Fig. 4 depicts the results of a full 2DDQ experiment obtained at 21°C for $^{23}Na^+$ present in cortical homogenate. A similar result was obtained for this ion present in nuclear homogenate (not shown). No indication of satellite resonances were apparent in the single quantum $^{23}Na^+$ spectra of either cortical or nuclear homogenates. Each double quantum filtered spectrum was simulated as a difference (antiphase) of two Lorentzian lineshapes differing in width. Because the two-dimensional data processing used in this study provided absolute value (magnitude) spectra, the assumption of a Lorentzian lineshape was not strictly valid. For cortical homogenate, the narrow component (line width = 24 Hz) accounted for 50.0% of the spectral intensity, whereas the broad component (line width = 241 Hz) made up the remainder of the observed $^{23}Na^+$ spectral intensity in accordance with theoretical expectations. For the nuclear homogenate the corresponding values were narrow, 48.0% (line width = 57 Hz), and broad, 52.0% (line width = 657 Hz). Each double quantum spectrum exhibited only one resonance; line widths at half-height were 182 and 490 Hz, respectively, for cortical and nuclear homogenates. Unfortunately, the corresponding full 2DDQ $^{39}K^+$ experiment was not

FIGURE 1 Simulated double quantum filtered NMR spectral lineshapes for an isolated $I = 3/2$ nucleus at 7.05 T as a function of correlation time. (*A*) $\tau_c = 5$ ns; (*B*) $\tau_c = 10$ ns; (*C*) $\tau_c = 50$ ns; (*D*) $\tau_c = 100$ ns. A quadrupolar coupling constant of 700 kHz was used for the simulations. The condition $\kappa \leq 1$ (reference 38) was fulfilled for each assumed correlation time. See text for theoretical expressions.

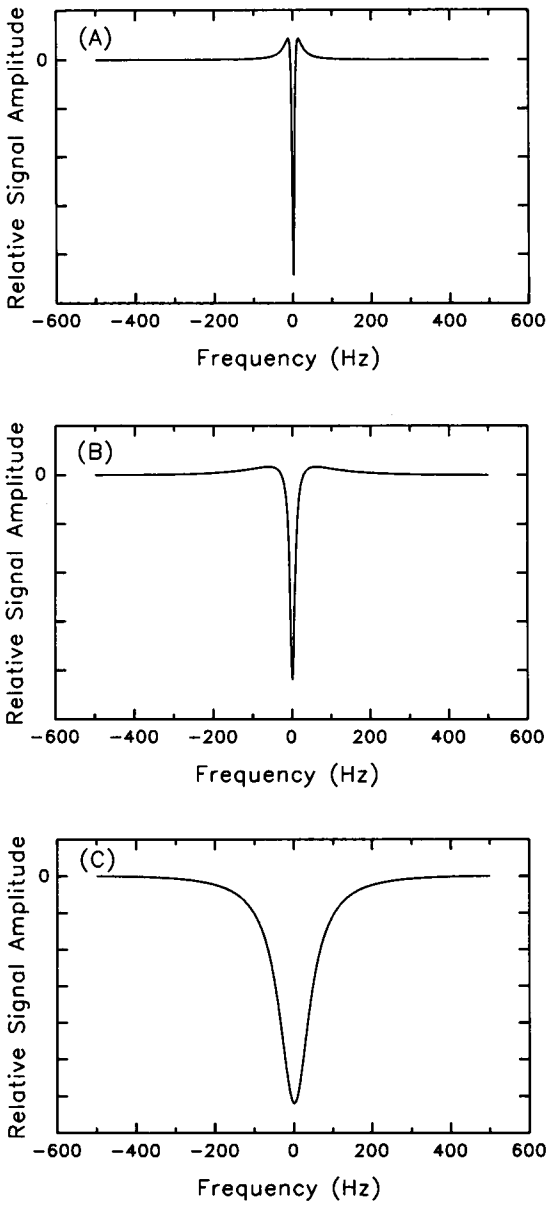

FIGURE 2 Simulated double quantum filtered NMR spectral lineshapes for an isolated $I = 3/2$ nucleus at 7.05 T in discrete two-site fast exchange between assumed "free" and "bound" states as a function of the bound mole fraction (Θ_B). (*A*) $\Theta_B = 0.001$; (*B*) $\Theta_B = 0.01$; (*C*) $\Theta_B = 0.1$. Correlation times of 0.01 and 10 ns and quadrupolar coupling constants of 700 kHz and 1.7 MHz were used to represent the "free" and "bound" states, respectively, for the simulations ($\kappa \leq 1$). See text for theoretical expression.

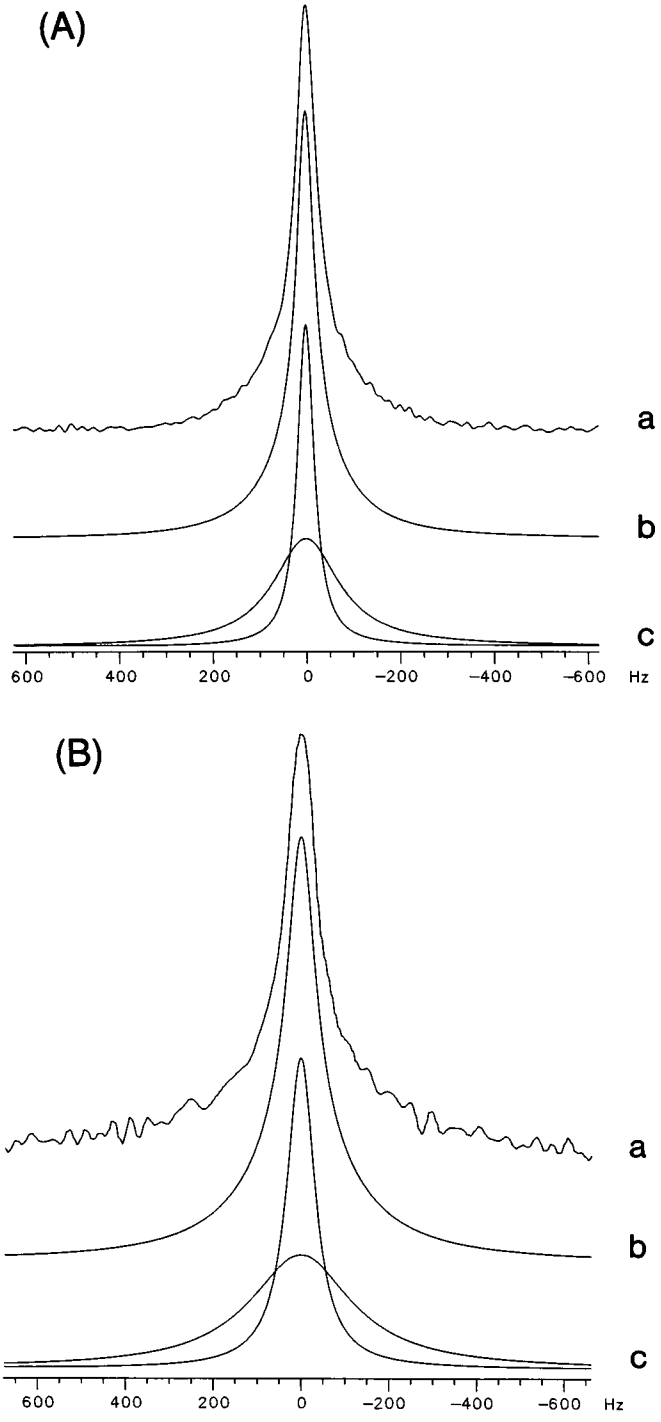

FIGURE 3 One pulse $^{39}K^+$ NMR spectra for (*A*) cortical ($[K^+] \approx 139$ mM) and (*B*) nuclear ($[K^+] \approx 127$ mM) calf lens homogenates. (*a*) experimental spectrum; (*b*) simulated spectrum (sum of broad and narrow spectral components obtained by spectral deconvolution); (*c*) deconvoluted broad and narrow spectral components. See text for spectral line-shape characteristics and Table 1 for spectral acquisition parameters. Temperature = 21.5°C.

feasible because of a low signal-to-noise ratio, necessitating a minimum of 4–5 d of spectral accumulation.

The rate constants characterizing quadrupolar ion magnetic relaxation were evaluated using several methods. These included HSVD analysis, nonlinear regres-

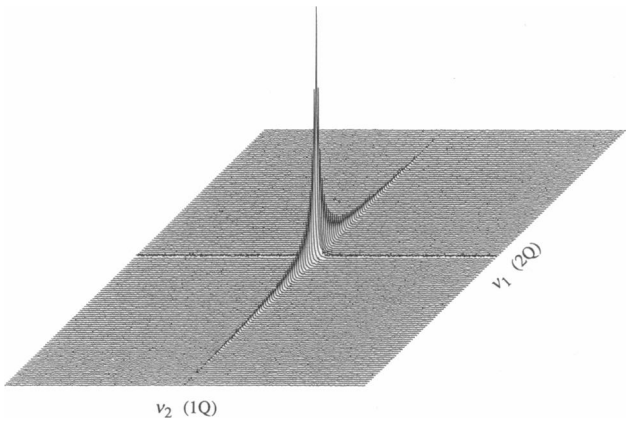

FIGURE 4 2DDQ $^{23}Na^+$ spectrum of calf lens cortical homogenate at 21°C. Acquisition parameters were as follows: sweepwidth (ν_2), ±6,250 Hz, sweepwidth (ν_1), ±12,500 Hz; acquisition time, 81.9 ms; repetition time, 182 ms, τ = 4.8 ms; number of acquisitions, 4800; 128 blocks; total time 29.4 h. See text and Table 1 for additional details.

sion, and linear regression of semilog representations of the relaxation data. Despite the nonLorentzian nature of the quadrupolar ion resonance absorption signals obtained for both cortical and nuclear homogenate preparations, the longitudinal magnetization in each case was observed to decay with a single apparent rate constant (R_{1lin}) in inversion recovery experiments. This was confirmed by HSVD analysis, which indicated only one relaxing component, and by the observation of linear semilog plots of inversion recovery magnetization data. Longitudinal relaxation rate constants (R_{1lin}) for both $^{23}Na^+$ and $^{39}K^+$ were found to be about two times larger in nuclear than cortical lens tissue homogenate. Similarly, R_{1lin} values for $^{39}K^+$ in both cortical and nuclear lens homogenates were found to be about two times greater than the corresponding values for $^{23}Na^+$. The values of the longitudinal relaxation rate constants for $^{23}Na^+$ and $^{39}K^+$ in cortical and nuclear homogenates are tabulated in Tables 2 and 3.

The longitudinal relaxation rate constant R_A for the free $^{23}Na^+$ ion in cortical and nuclear lens homogenate, assuming a two-site discrete fast exchange model, was calculated by solving the set of equations for R_{1lin} (Eq. 3c) using relaxation data obtained at 79.5 and 132.28 MHz. For these particular preparations at 23.7°C the following R_{1lin} values were obtained: 132.28 MHz: 44.8 ± 0.3 s^{-1} (cortical), 79.7 ± 1.4 s^{-1} (nuclear); 79.5 MHz: 49.3 ± 0.4 s^{-1} (cortical), 93.5 ± 1.6 s^{-1} (nuclear). Calculated relaxation rate constant values for "free" $^{23}Na^+$ in cortical and nuclear lens homogenates of 42.3 ± 0.7 and 72.0 ± 3.0 s^{-1}, respectively, were obtained. Because relaxation measurements for $^{39}K^+$ were only performed at 7.05 Tesla the assumption was made that the experimentally observed ratio of the ionic T_1 values in water ($^{23}Na^+$[20 mM/$^{39}K^+$[150 mM] = 0.972) at 7.05 T was applicable to the lens homogenate situation. Values of 43.5 ± 0.7 and 74.0 ± 3.1 s^{-1} in cortical and nuclear homogenates, respectively, were calculated for "free" $^{39}K^+$.

HSVD analysis indicated the presence of only two antiphase relaxing magnetization components with $R_{2F}/R_{2S} > 4.4$ for $^{39}K^+$ (≈450 mM) and > 10 for $^{23}Na^+$ (≈20 mM) in double quantum filtered experiments. Such separation of the two relaxation processes was more than sufficient to permit biphasic data analysis. The slower relaxing fraction was analyzed first, using data obtained after the fast relaxation process was essentially completed, and R_{2S} was extracted by linear regression of semilog plots which were linear for at least 2.5 half-lives. Adopting a value of τ_{ref} such that $\exp(-\tau_{ref}R_{2F}) \cong 0$ allowed the rearrangement of Eq. 7 to Eq. 13, from which R_{2F} may be determined.

$$\ln\{\exp(-\tau R_{2S}) - S_{rel}\exp[(-\tau_{ref})R_{2S}]\} = -R_{2F}\tau. \quad (13)$$

Examples of plots from which the rate constants were obtained by nonlinear regression analysis, using Eq. 5, of the relative signal intensity obtained as a function of τ in a 1DDQ experiment for the two ions present in cortical and nuclear homogenates are shown in Figs. 5 *A* and *B*, respectively. The solid lines in Figs. 5 and 6 were

TABLE 2 $^{23}Na^+$ and $^{39}K^+$ NMR relaxation parameters for bovine lens cortical homogenate at 7.05 T

Relaxation parameter	$^{23}Na^+$	$^{39}K^+$
R_{1lin}	54.2 ± 0.5 s^{-1}	107.4 ± 0.4 s^{-1}
R_{2S}	56.5 ± 0.1	142 ± 4
R_{2F}	587 ± 3	627 ± 19
R^{2Q}	562 ± 11	638 ± 10
α	10.2	4.4
τ_{opt}	4.5 ms	3.1 ms

$[Na^+] \approx 20$ mM, $[K^+] \approx 450$ mM.

TABLE 3 $^{23}Na^+$ and $^{39}K^+$ NMR relaxation parameters for bovine lens nuclear homogenate at 7.05 T

Relaxation parameter	$^{23}Na^+$	$^{39}K^+$
R_{1lin}	95.2 ± 0.3 s^{-1}	226.6 ± 0.2 s^{-1}
R_{2S}	98.7 ± 1.5	272 ± 22
R_{2F}	1570 ± 20	1544 ± 149
R^{2Q}	1530 ± 20	1386 ± 27
α	16	5.7
τ_{opt}	1.9 ms	1.4 ms

$[Na^+] \approx 20$ mM, $[K^+] \approx 450$ mM.

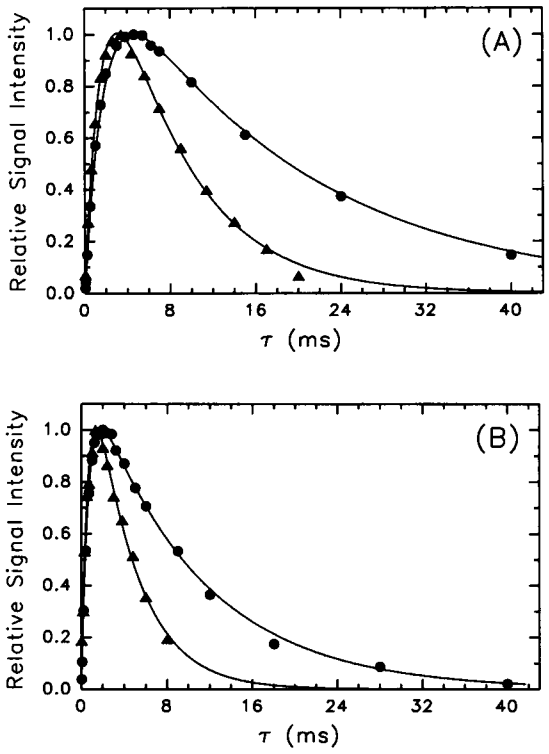

FIGURE 5 1DDQ $^{23}Na^+$ and $^{39}K^+$ relative signal intensity vs. preparation time (τ) plots obtained for cortical and nuclear lens homogenates at 21.5°C. (*A*) cortical homogenate (●) $^{23}Na^+$ (≈20 mM) and (▲) $^{39}K^+$ (≈450 mM). (*B*) nuclear homogenate (●) $^{23}Na^+$ (≈20 mM) and (▲) $^{39}K^+$ (≈450 mM). Spectral acquisition parameters are listed in Table 1.

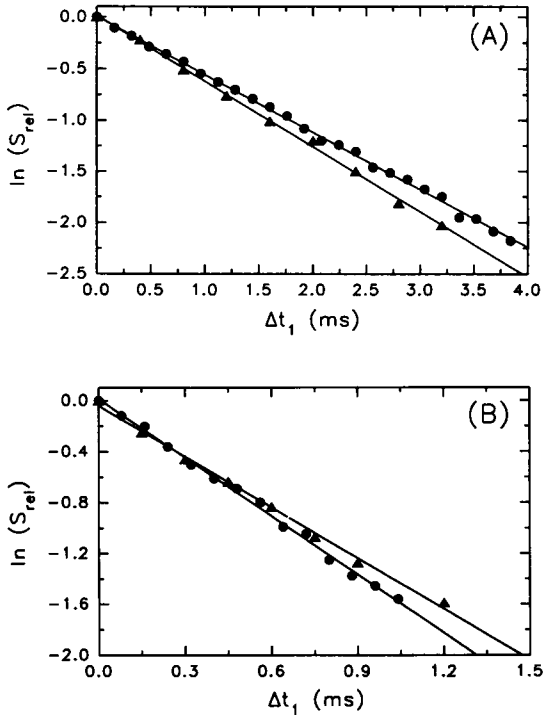

FIGURE 6 Ln S_{rel} vs. evolution time (Δt_1) obtained from a 1DDQ experiment for cortical and nuclear lens homogenates at 21.5°C. (*A*) cortical homogenate (●) $^{23}Na^+$ (≈20 mM) and (▲) $^{39}K^+$ (≈450 mM). (*B*) nuclear homogenates (●) $^{23}Na^+$ (≈20 mM) and (▲) $^{39}K^+$ (≈450 mM). The slope is equal to $-R^{2Q}$. The spectrum with the smallest t_1 was used as the reference.

calculated theoretically by using the values of R_{2S} and R_{2F} obtained by nonlinear regression analysis. The values of the relaxation rate constants R_{2S} and R_{2F} are tabulated in Table 2. Virtually identical values for R_{2S} and R_{2F} were obtained by employing Eq. 13 and linear regression. In all cases, the relaxation rate constant values were larger in nuclear than cortical homogenate by about a factor of two. For R_{2S}, values for $^{39}K^+$ were found to be about two times greater than those for $^{23}Na^+$. By contrast, for R_{2F}, the values obtained for $^{23}Na^+$ and $^{39}K^+$ were virtually the same.

Fig. 6 shows an example of the decay of double quantum coherence, represented by the rate constant R^{2Q}, which was obtained from pseudo 2DDQ experiments. HSVD analysis indicated the presence of only one relaxing component in each case examined. R^{2Q} was calculated from plots of natural logarithm of the relative signal intensity [ln (S_{rel})] as a function of the evolution time (Δt_1) using Eq. 8. Evolution times (t_1) were varied from several microseconds to a few milliseconds, thus allowing observation of double quantum coherence decay over a period of about three half-lives. Both $^{23}Na^+$ (≈20 mM) and $^{39}K^+$ (≈450 mM) have similar double-quantum decay rates in cortical and nuclear homogenate. However, the values of the relaxation rate constants are two to three times greater in nuclear than cortical homogenate. The values are tabulated in Tables 2 and 3.

The lifetime of the "bound" ions was determined by using several different methods. The first method employed the general approach of Rose and Bryant (47), which assumed a discrete two-site fast exchange binding model, in which a theoretical ratio of excess relaxation rates was calculated as a function of the correlation time for the "bound" ion ($\tau_{c,B}$), and the experimental value of the excess relaxation rate was in turn used to determine $\tau_{c,B}$. In the theoretical calculations (Eqs. 3–5), quadrupolar coupling constants of 0.7 and 1.7 MHz were used for the "free" and "bound" states (48, 49) of $^{23}Na^+$, respectively, whereas the corresponding values adopted for $^{39}K^+$ were 0.73 and 1.77 MHz, respectively, for the "free" and "bound" ionic forms. The values for the $^{39}K^+$ quadrupolar coupling constants were estimated by scaling the solution $^{23}Na^+$ quadrupolar coupling constant values by a factor (1.04) obtained by taking an average of

TABLE 4 $^{23}Na^+$ and $^{39}K^+$ NMR and binding parameters for bovine lens homogenates obtained from fitting experimental relaxation data assuming discrete two-site and asymmetric distribution models

	Cortical		Nuclear	
	$^{23}Na^+$	$^{39}K^+$	$^{23}Na^+$	$^{39}K^+$
Discrete two-site model				
$\tau_{c,B}$ (ns)	14 ± 3	29.3 ± 2.5	14 ± 3	29.3 ± 2.5
χ_A (MHz)	0.7	0.73	0.7	0.73
χ_B (MHz)	1.7	1.77	1.7	1.77
Θ_A	0.994	0.997	0.983	0.993
Θ_B	0.006	0.003	0.017	0.007
RMS error (%)	9.3	11.9	8.4	13.1
	$^{23}Na^+$	$^{39}K^+$	$^{23}Na^+$	$^{39}K^+$
Asymmetric distribution* model				
a	4.57	0.96	1.41	4.57
b	0.154	0.282	0.145	0.194
χ (MHz)	0.52	0.33	0.59	0.23
τ_m (ps)	0.107	80.0	0.195	87.1
RMS error (%)	10.9	18.7	11.5	8.5

*Limits employed in the fits: *a*, 0.8–5.0; *b*, 0.09–0.4; χ = 0.2–2.0 MHz; τ_m = 0.1–100.0 ps.

the ratio of T_1 values for dilute aqueous solutions of NaCl and KCl ($^{23}Na^+/^{39}K^+$ = 0.972) and the ratio of alkali-metal halide quadrupolar coupling constants in the gas phase (NaCl/KCl = 0.953) (50, 51). Experimental excess relaxation rate ratios defined by $(R_X - R_A)/(R_{1lin} - R_A)$, where R_X represents either R_{2F} or R^{2Q} were compared with the corresponding theoretical values. The results are tabulated in Table 4. Average values of 14 ± 3 ns for $^{23}Na^+$ and 29.5 ± 1.5 ns for $^{39}K^+$ were obtained for the correlation times of these ions in both cortical and nuclear homogenates at 21°C. The fraction of "bound" ion was in turn calculated using the expression for R_{2F} (Eqs. 3, 4, 9). In this case the experimental values of R_{2F} and R_A, the calculated values of $\tau_{c,B}$, and an assumed value of 1.7 MHz for the quadrupolar coupling constant of the bound ion were used (48, 49). Θ_B values of 0.006 and 0.017 for $^{23}Na^+$ and 0.003 and 0.007 for $^{39}K^+$ were obtained for cortical and nuclear homogenates, respectively, at 21°C.

The second method employed also assumed a discrete two-site binding model and involved iterative least-square matching of theoretical single and double quantum filtered spectral line shapes to the corresponding experimental spectra (calculated using the experimentally determined relaxation rate constants and spectral acquisition parameters) employing $\tau_{c,B}$ and Θ_B as variables. R_A, which represents the relaxation rate constant for "unbound" ion, was set to the experimentally determined value for cortical or nuclear homogenate (vide supra). The relevant relaxation rate constants were calculated according to Eqs. 3, 4, and 9 and Eqs. 2 and 5 were Fourier transformed (1,024 data points) to yield single and double quantum filtered spectra, respectively. Correlation time values of 15 ± 1 and 16 ± 1 ns were obtained for cortical and nuclear homogenates. Values of the fraction of "bound" Na^+ were 0.006 and 0.016 for cortical and nuclear homogenates, respectively, at 21°C.

The derived values of $\tau_{c,B}$, Θ_B, and R_A were used to calculate the entire suite of ionic relaxation rate constants characterizing discrete two-site binding by employing Eqs. 3, 4, and 9. A root mean square error was in turn calculated by using both the calculated and experimental individual relaxation rate constant values. The obtained errors for $^{23}Na^+$ and $^{39}K^+$ discrete two-site binding are listed in Table 4. This procedure is analogous to the plots (ν_Q^{rms} [= $\omega_Q^{rms}/2\pi$] vs log τ_c) introduced by Rooney and Springer (33, 34), in which the intersection points of the individual relaxation rate curves with each other define a "circle of confusion," the radius of which is used as a criterion of the appropriateness of the discrete two-site fast exchange model.

The final method employed for the analysis of quadrupolar ion relaxation data assumed a distribution of ionic correlation times, $p(\tau_c)$. In this model the experimental values obtained for R_{1lin}, R_{2S}, R_{2F}, and R^{2Q} were used, and four adjustable parameters were employed for the fits: the widths of the discontinuous distribution (*a* and *b*), the modal value of the correlation time (τ_m), and the quadrupolar coupling constant (χ). Correlation time distribution curve plots for $^{23}Na^+$ and $^{39}K^+$ in cortical and nuclear lens homogenates are shown in Figs. 7 *A* and *B*. For both ions, changes in protein concentration do not significantly affect the correlation time distribution curve. However, there are differences between the $^{23}Na^+$ and the $^{39}K^+$ distribution curves, the most pronounced being the modal point, τ_m. This suggests that the major difference between the two ions is the correlation time of the "free" ion. The parameters characterizing the distribution model for $^{23}Na^+$ and $^{39}K^+$ relaxation data are summarized in Table 4.

NMR visibility studies

The total average concentrations of sodium determined by atomic absorption were 26.3 ± 1.0 mM in the cortex and 19.5 ± 0.5 mM in the nucleus. The respective NMR visible sodium concentrations were 24.9 ± 3.5 mM for the cortex and 17.5 ± 1.0 mM for the nucleus. For the potassium ion, atomic absorption measurements for the cortex and nucleus yielded 139.0 ± 4.0 and 126.5 ± 6.5 mM, respectively. The corresponding NMR measurements were 120 ± 10 and 130 ± 14 mM, respectively. The derived NMR visibility factors and their standard errors are tabulated in Table 5. The atomic absorption

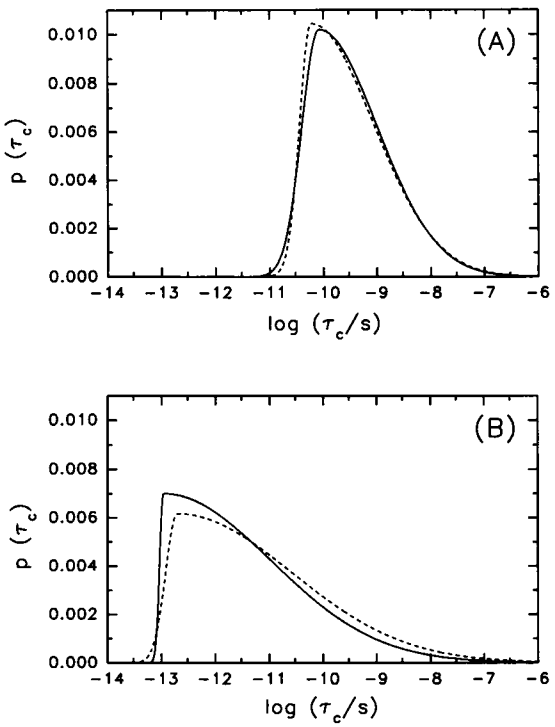

FIGURE 7 Asymmetric log-gauss correlation time distribution plots obtained for $^{39}K^+$ and $^{23}Na^+$ in bovine cortical and nuclear lens homogenates. (*A*) $^{39}K^+$, cortical (——) and nuclear (– – –) homogenates. (*B*) $^{23}Na^+$, cortical (——) and nuclear (– – –) homogenates. Parameters defining each distribution are listed in Table 4.

and NMR results clearly indicate that sodium is found predominantly in the cortical regions of the lens, whereas potassium appears to be more evenly distributed. These values are all within the range typically reported in the literature (15). Qualitatively the results also show that the majority of Na^+ and K^+ present in lens homogenates is free. However, because of the relatively large uncertainties in the measurements it is difficult to clearly define the precise amounts of NMR invisible ion.

DISCUSSION

The experiments described in this paper were performed to further the understanding of spin ½ quadrupolar ion behavior in the intracellular state as exemplified by the crowded protein environment of eye lens homogenate. Single and double quantum NMR experiments indicate that the magnetic relaxation behavior of $^{23}Na^+$ and $^{39}K^+$ in bovine cortical and nuclear lens homogenates is homogeneous biexponential (type *c*). For $^{39}K^+$ R_{1lin} and R_{2S} values were two to three times greater than those of $^{23}Na^+$, whereas the values for R_{2F} and R^{2Q} were approximately the same. The observation that $R_{1lin} \approx R_{2S} \ll R_{2F} \approx R^{2Q}$ and $R_{1lin} < R_{2S} \ll R_{2F} \approx R^{2Q}$ for $^{23}Na^+$ and $^{39}K^+$, respectively, is diagnostic of correlation time heterogeneity, which includes contributions from both the extreme motionally narrowed ($\omega_L\tau_c \ll 1$) and nonextreme motionally restricted ($\omega_L\tau_c \gg 1$) states. Short τ_c values are most likely associated with "free" ion behavior, whereas longer τ_c values are a reflection of more restricted motion, such as that arising from a fraction of ion bound to lens protein, or at least situated in the vicinity of negatively charged amino acid residues of cellular protein. In the context of the discrete two-site fast exchange model this fraction is designated as "bound." The occurrence of fast exchange (relative to the relaxation timescale) between different ion environments is evident from the observation that all the longitudinal magnetization decays with the same rate as opposed to two populations with different R_{1lin} values, as demonstrated by HSVD analysis. This conclusion is supported by HSVD analysis of the double quantum filtered relaxation data acquired in this study. If the exchange were slow, each population would give rise to a separate relaxation contribution that would decay with its own characteristic rate constant. The relaxation rate constants of both ions were found to be several-fold higher in nuclear than in cortical homogenate, thereby illustrating a dependence of these parameters on protein concentration.

As noted above, two different models were adopted for the analysis of the quadrupolar ion relaxation data. The first was a discrete two-site fast exchange model in which an ion may be found in either of two environments, "free" or "bound." The second, by contrast, assumed an asymmetric Gaussian distribution of correlation times. A convenient way of representing the distribution model is to imagine a three-dimensional lattice whose cells may be occupied by protein amino acid residues, ions, or solvent molecules. This view follows the liquid lattice theory developed by Flory (52) for the statistical thermodynamic treatment of polymer solutions. More specifically, the polypeptide backbone amino acid residues are situated in contiguous liquid lattice cells. Each empty lattice cell may be occupied by an ion or a water molecule. Thus, ions may be spatially located close to, at intermediate distances, or remotely from the protein chain, i.e., distributed over the available lattice

TABLE 5 NMR visibility factors for $^{23}Na^+$ and $^{39}K^+$ in bovine lens homogenates

Ion	Cortex	Nucleus
$^{23}Na^+$	0.95 ± 0.17	0.90 ± 0.05
$^{39}K^+$	0.86 ± 0.10	1.03 ± 0.16

space. The proximity of an ion to the polypeptide chain segments therefore defines its relaxation characteristics. Fast exchange is assumed to occur for the exchange of an ion from one lattice cell to another.

Analysis of the ionic relaxation data using the discrete two-site fast exchange model indicates that the majority of intralenticular $^{23}Na^+$ and $^{39}K^+$ is "free." Increasing protein concentration, such as that encountered in a cortical-to-nuclear environmental transition, does not lead to a change in the correlation time of the "bound" state, but only to an increase of the fraction of "bound" ion, Θ_B. Moreover, the correlation time of the "bound" state of $^{39}K^+$ was found to be approximately twice that of $^{23}Na^+$. The reason for this increase is currently not known.

Application of the correlation time distribution model to the relaxation data yields correlation time distribution curves. As shown in Fig. 7 *A*, the modal value for $^{39}K^+$ correlation time is about three orders of magnitude greater than that found for $^{23}Na^+$ (Fig. 7 *B*). Increasing protein concentration appears to have only a slight effect on the characteristics of the distribution curve, which is somewhat unexpected in view of the adopted lattice model. For the distribution model an average correlation time can be calculated for the species by using $\tau_c > \omega_L^{-1}$ (2 ns at the spectrometer frequency used) to crudely represent the division between the "free" and "bound" states. Values of $\sim$33 and 43 ns were obtained for cortical and nuclear homogenates for $^{23}Na^+$, whereas 48 $\pm$ 2 ns for both homogenates was obtained for $^{39}K^+$. Similarly, the fraction of "bound" ion falling in the range $\tau_c > \omega_L^{-1}$ may also be approximately calculated. Typically values of ≤ 0.05 were obtained, indicating that both ions are predominantly "free."

The longer correlation time obtained for the "bound" state of $^{39}K^+$ relative to the corresponding value of $^{23}Na^+$ is not likely due to the assumption that the ratios of the quadrupolar interactions and of the T_1 values of $^{39}K^+$ and $^{23}Na^+$ in lens homogenate are the same as in aqueous solution, because this assumption was only employed in the two-site analysis and not in the distribution model analysis.

The application of both the discrete two-site fast exchange and the distribution models to the experimental ion relaxation data result in approximately equal root mean square (RMS) error. Both yield equivalent qualitative information about the behavior of quadrupolar ions in a crowded protein environment. Until further experimental information is acquired there is no firm basis to favor one model over the other. A detailed analysis and discussion of the merits and pitfalls of both models is addressed in detail by Rooney and Springer (33, 34).

The minimum average correlation time for lens protein reorientational motion is $\sim$100 ns at 18°C in both cortical and nuclear homogenates (53). The values obtained for the ions depend, as noted above, on the type of model used to analyze the data. In either case, the value for protein reorientational motion is much larger than that obtained for the correlation times of the "bound" ions and suggests that a process faster than protein reorientational motion is dominating the "bound" state. Two likely candidates are chemical exchange from the "bound" to the "free" state and the occurrence of protein internal motion at the protein binding sites. The latter is probably unlikely because internal motion of proteins occurs on a subnanosecond timescale. This is further supported by the observation that the correlation times of the "bound" ions are similar for the cortical (lower protein concentrations) and nuclear (higher protein concentrations), suggesting that $\tau_{c,B}$ is independent of solvent viscosity. Because the protein rotational motion depends, in part, on solvent viscosity, the above observations are most likely manifestations of the occurrence of a fast (relative to protein reorientational motion) kinetic process dominating the overall correlation time. Unfortunately, a consequence of this is that little information, if any, can be inferred about lens protein motion or interaction from $^{23}Na^+$ and $^{39}K^+$ quadrupolar ion relaxation data.

Previous dialysis studies on the efflux of $^{23}Na^+$ from human lenses (21) indicated that the lenticular sodium ions are relatively "free" and in a mobile state in both clear and cataractous lenses. In addition, these studies revealed the presence of a small fraction ($\sim$0.02) of nondiffusible, i.e., nonexchangeable sodium. The conclusions of the present NMR study, namely the occurrence of a predominantly "free" and mobile ion population, and the likelihood of at least some NMR invisible ionic populations, is in agreement with the interpretation of an essentially "free" and mobile state for lens sodium and potassium offered by Duncan and van Heyningen (21, 54). However, the small fraction of nondiffusible sodium detected in these studies (21) should not be confused with the small fraction of rapidly exchanging "bound" ion contributing to the NMR spectral and relaxation behavior (discrete two-site model assumed). In the absence of exchange, the small amount of "bound" sodium would not be readily detectable by NMR methods, not only because of the small fractional population size, but also because of the extremely short T_2 of the "bound" component. The upper limit of the short T_2 of "bound" nonexchangeable $^{23}Na^+$ is $\sim$11 μs, and can be obtained from the value $(R_{2F})_B \cong 9 \times 10^4\ s^{-1}$, which was determined in this study for both cortical and nuclear lens homogenates (the actual T_{2F} of nonexchangeable ion can be orders of magnitude $<$11 μs). On the other hand, small fractions of "bound" exchangeable ions become detectable because their presence is ampli-

fied by rapid exchange, a conclusion supported by spectral simulations. The mechanism of this amplification effect can be understood by considering the physical meaning of Eq. 9. Thus, the relationship $\Theta_A R_A \gg \Theta_B(R_{2S})_B$ (Eq. 9) underscores the notion that the central Zeeman transition of lens ions relaxes mainly through fluctuations that occur at the free site. By contrast, the relationship $\Theta_A R_A \ll \Theta_B(R_{2F})_B \sim \Theta_B(R^{2Q})_B$ (Eq. 9) suggests that the satellite and double quantum transitions relax primarily by way of fluctuations in the vicinity of macromolecules, after the ion has undergone chemical exchange. The preference for relaxation as a "bound" ion reflects the dominance of the kinetic $[R_A \ll (R_{2F})_B]$ over the thermodynamic effect ($\Theta_A \gg \Theta_B$). Thus, it becomes apparent from this analysis that multiple quantum coherence can be excited not only from spins exhibiting type *a*, *b*, and *c* behavior but also from a type *d* (3) population, in fast exchange with environments of reduced motion (e.g., type *c*).

Studies with freeze-fractured lenses revealed that the macroscopic translation diffusion coefficient for Na^+ is about one-third that of the free solution value, whereas the corresponding value for Ca^{2+}, an ion known to bind tightly to lens proteins, has a value of about one-tenth that in free solution (55). Other studies (for a review see reference 55) demonstrated an anomalous (slow) diffusion behavior of Na^+ through the lens. By contrast, K^+ and Rb^+ penetrate lens tissue rapidly. Duncan (56) attributed this to the specific interaction of Na^+ with fixed negative charges in the lens, most likely solvent exposed carboxyl groups of lens proteins. The results of this NMR study indicate that the anomalous diffusion behavior of lenticular Na^+ cannot be attributed solely to significant interaction with lens macromolecular constituents.

It is generally acknowledged that the activity coefficients of Na^+ in the cytoplasm of many tissues, including the lens, is very low (~ 0.2), whereas that of K^+ is much closer to the aqueous solution value (0.8) (55, 57). Measurements of Na^+ and K^+ activity coefficients in concentrated bovine serum albumin solutions (58) indicate that a decrease of $\sim 12\%$ from the protein-free solution occurs ($\gamma = 0.7$) at a protein concentration of $\sim 21\%$. Similar values were reported for these ions in concentrated hemoglobin solutions (58). The interpretation of these thermodynamic studies is that the activity coefficient of simple salts in concentrated protein solutions depends primarily on the extent of anion binding and on the amount of bound water. A drastically decreased value of the apparent activity coefficient of an ion would imply sequestration. Such an interpretation is not supported by the NMR results for lens tissue reported in this paper, by macroscopic diffusion measurements in freeze-fractured lenses (55), and by thermodynamic measurement of ion activity coefficients in concentrated protein solutions (58), thereby suggesting the need for a reevaluation of the activity coefficient of sodium in lens tissue. The results of this study also suggest that the majority of the intracellular sodium and potassium is "free" and thus able to affect the intralenticular water chemical potential.

We thank the University of California at Davis NMR Facility for providing time on their GE GN-500 spectrometer, Professor Ilan Benjamin for valuable suggestions regarding distribution curve simulation computer programs, and Jim Loo for NMR technical assistance.

This research was supported by National Institutes of Health grant EY 04033.

Received for publication 9 August 1991 and in final form 12 November 1991.

REFERENCES

1. Harding, J. J., and M. J. C. Crabbe. 1984. The lens: development, proteins, metabolism, and cataract. *In* The Eye. Vol. 1B. 3rd ed. H. Davson, editor. Academic Press, London, 1B, 207–492.
2. Duncan, G. 1974. Comparative physiology of lens membranes. *In* The Eye. Vol. 5. H. Davson and L. T. Graham, Jr., editors. Academic Press, London, 357–398.
3. Rooney, W. D., T. M. Barbara, and C. S. Springer, Jr. 1988. Two-dimensional double-quantum NMR spectroscopy of isolated spin ½ systems: ^{23}Na examples. *J. Am. Chem. Soc.* 110:674–681.
4. Springer, C. S., Jr. 1987. Measurement of metal cation compartmentation in tissue by high resolution metal cation NMR. *Annu. Rev. Biophys. Biophys. Chem.* 16:375–399.
5. Springer, C. S., Jr. 1988. ^{23}Na and ^{39}K NMR spectroscopic studies of the intact, beating, heart. *In* Study of Cardiovascular Problems with NMR Techniques. M. Osbakken, editor. Futura Publishing Co., Mt. Kisco, NY. 218–319.
6. Civan, M. M., and M. Sphorer. 1978. NMR of sodium-23 and potassium-39 in biological systems. *In* Biological Magnetic Resonance. Vol. 1. L. J. Berliner and J. Reuben, editors. Plenum Press, New York. 1–32.
7. Payne, G. S., A.-M. L. Seymour, P. Styles, and G. K. Radda. 1990. Multiple quantum filtered ^{23}Na NMR spectroscopy in the perfused heart. *NMR Biomed.* 3:139–145.
8. Allis, J., A.-M. L. Seymour, and G. K. Radda. 1991. Absolute quantification of intracellular Na^+ using triple-quantum filtered sodium-23 NMR. *J. Magn. Reson.* 93:71–76.
9. Shinar, H., and G. Navon. 1991. Sodium-23 NMR relaxation times in nucleated red blood cells and suspensions of nuclei. *Biophys. J.* 59:203–208.
10. Seo, Y., M. Murakami, E. Suzuki, S. Kuki, K. Nagayama, and H. Watari. 1990. NMR characteristics of intracellular K in the rat salivary gland: a ^{39}K NMR study using double-quantum filtering. *Biochemistry.* 29:599–603.
11. Hiraishi, T., Y. Seo, M. Murakami, and H. Watari. 1990. Detection of biexponential relaxation in intracellular K in the rat heart by double-quantum ^{39}K NMR. *J. Magn. Reson.* 87:169–173.

12. Lyon, R. C., J. Pekar, C. T. W. Moonen, and A. C. McLaughlin. 1991. Double-quantum surface-coil NMR studies of sodium and potassium in the rat brain. *Magn. Reson. Med.* 18:80–92.

13. Allis, J. L., R. M. Dixon, A. M. Till, and G. K. Radda. 1989. $^{87}Rb^+$ NMR studies for evaluation of K^+ fluxes in human erythrocytes. *J. Magn. Reson.* 85:524–529.

14. Allis, J. L., R. M. Dixon, and G. K. Radda. 1990. A study of transverse relaxation of $^{87}Rb^+$ in agarose gels by triple-quantum filtration. *J. Magn. Reson.* 90:141–147.

15. Paterson, C. A. 1969. Distribution of sodium and potassium in ox lenses. *Exp. Eye Res.* 8:442–446.

16. Bonting, S. L., L. L. Caravagg, and N. M. Hawkins. 1963. Studies on sodium–potassium activated adenosine triphosphate. VI. Its role in cation transport in the lens of cat, calf, and rabbit. *Arch. Biochem. Biophys.* 101:47–55.

17. Kinsey, S. E., and D. V. N. Reddy. 1965. Studies on the crystallin lens. XI. The relative role of the epithelium and capsule in transport. *Invest. Ophthalmol.* 4:104–116.

18. Reddy, D. V. N. 1979. Dynamics of transport systems in the eye. *Invest. Ophthalmol.* 18:1000–1018.

19. Pettegrew, J. W., T. Glonek, N. J. Minshew, and D. E. Woessner. 1985. Sodium-23 NMR of intact bovine lens and vitreous humor. *J. Magn. Reson.* 63:439–444.

20. Garner, W. H., S. K. Hilal, S.-W. Lee, and A. Spector. 1986. Sodium-23 magnetic resonance imaging of the eye and lens. *Proc. Natl. Acad. Sci. USA.* 83:1901–1905.

21. Duncan, G., and R. van Heyningen. 1977. Distribution of non-diffusible calcium and sodium in normal and cataractous lenses. *Exp. Eye Res.* 25:183–193.

22. Chang, D. C., and D. E. Woessner. 1978. Spin echo study of ^{23}Na relaxation in skeletal muscle. Evidence of sodium ion binding inside a biological cell. *J. Magn. Reson.* 30:185–191.

23. Shinar, H., and G. Navon. 1986. Sodium-23 NMR relaxation times in body fluids. *Magn. Reson. Med.* 3:927–934.

24. Berendsen, H. J. C., and H. T. Edzes. 1973. The observation and general interpretation of sodium magnetic resonance in biological material. *Ann. NY Acad. Sci.* 204:459–485.

25. Pekar, J., P. F. Renshaw, and J. S. Leigh, Jr. 1987. Selective detection of intracellular sodium by coherence-transfer NMR. *J. Magn. Reson.* 72:159–161.

26. Pekar, J., and J. S. Leigh, Jr. 1986. Detection of biexponential relaxation in sodium-23 facilitated by double quantum filtering. *J. Magn. Reson.* 69:582–584.

27. Jelicks, L., and R. J. Gupta. 1989. Observation of intracellular sodium ions by double quantum filtered Na-23 NMR with paramagnetic quenching of extracellular coherence by gadolinium tripolyphosphate. *J. Magn. Reson.* 83:146–151.

28. Jaccard, G., S. Wimperis, and G. Bodenhausen. 1986. Multiple quantum NMR spectroscopy of $S = 3/2$ spins in isotropic phase: a new probe for multiexponential relaxation. *J. Chem. Phys.* 85:6282–6293.

29. Hubbard, P. S. 1970. Nonexponential nuclear magnetic relaxation by quadrupole interactions. *J. Chem. Phys.* 53:985–987.

30. Bull, T. E. 1972. Nuclear magnetic resonance of spin 3/2 nuclei involved in chemical exchange. *J. Magn. Reson.* 8:344–353.

31. Payne, G. S., P. Styles, and G. K. Radda. 1989. Applications of multiple quantum filtered ^{23}Na MRS in biological systems. *Soc. Magn. Reson., 8th Annu. Meet. Abstr.* 2:255.

32. Marshall, A. G. 1970. Calculation of NMR relaxation times for quadrupolar nuclei in the presence of chemical exchange. *J. Chem. Phys.* 52:2527–2534.

33. Rooney, W. D., and C. S. Springer, Jr. 1991. A comprehensive approach to the analysis and interpretation of the resonances of spins 3/2 from living systems. *NMR Biomed.* 4:209–226.

34. Rooney, W. D., and C. S. Springer, Jr. 1991. The molecular environment of intracellular sodium: ^{23}Na NMR relaxation. *NMR Biomed.* 4:227–245.

35. Hertz, H. G. 1983. The problem of intramolecular rotation in liquids and nuclear magnetic relaxation. *Prog. NMR Spect.* 16:115–162.

36. Fedotov, V. D., and H. Schneider. 1989. Structure and dynamics of bulk polymers by NMR methods. *NMR Basic Prin. Prog.* 21:1–176.

37. Merbolt, K.-D., and J. Frahm. 1986. ^1H-NMR relaxation study of water in binary solvent mixtures in the absence and presence of electrolytes. *Ber. Bunsen-Ges. Phys. Chem.* 90:614–621.

38. Ellev, U., and G. Navon. 1990. Criteria for multiexponential relaxation of exchanging spin-3/2 nuclei. *J. Magn. Reson.* 88:223–240.

39. Morgan, C. F., T. Schleich, G. H. Caines, and P. N. Farnsworth. 1989. Elucidation of intermediate (mobile) and slow (solidlike) protein motions in bovine lens homogenates by carbon-13 NMR spectroscopy. *Biochemistry.* 28:5065–5074.

40. Ernst, R. R., G. Bodenhausen, and A. Wokaun. 1987. Principles of Nuclear Magnetic Resonance in One and Two Dimensions. Oxford University Press, Oxford, U.K. 242–252.

41. Bax, A., R. Freeman, S. P. Kempsell. 1980. Natural abundance ^{13}C–^{13}C coupling observed via double quantum coherence. *J. Am. Chem. Soc.* 102:4849–4851.

42. Bax, A. 1984. Two Dimensional Nuclear Magnetic Resonance in Liquids. Delft University Press, Delft, The Netherlands. 129–154.

43. Barkhuijsen, H., R. de Beer, W. M. M. J. Bovee, and D. van Ormondt. 1985. Retrieval of frequencies, amplitudes, damping factors, and phases from time domain signals using a linear least squares procedure. *J. Magn. Reson.* 61:465–481.

44. Barkhuijsen, H., R. de Beer, and D. van Ormondt. 1987. Improved algorithm for noniterative time domain model fitting to exponentially damped magnetic resonance signals. *J. Magn. Reson.* 73:553–557.

45. Yan, H., and J. C. Gore. 1988. The relation of HSVD to LPSVD for fitting time domain signals. *J. Magn. Reson.* 80:324–327.

46. Daniel, C., and F. S. Wood. 1980. Fitting Equations to Data. 2nd ed. John Wiley & Sons, New York. 420–447.

47. Rose, K., and R. G. Bryant. 1978. Electrolyte ion correlation times at protein binding sites. *J. Magn. Reson.* 31:41–47.

48. Shinar, H., and G. Navon. 1984. NMR relaxation studies of intracellular Na^+ in red blood cells. *Biophys. Chem.* 20:275–283.

49. Cornelis, A., and P. Laszlo. 1979. Sodium binding sites of gramicidin A: sodium-23 nuclear magnetic resonance study. *Biochemistry.* 18:2004–2007.

50. van Wachem, R., and A. Dymanus. 1967. Radiofrequency spectra of KF and KCl by the molecular-beam electric-resonance method. *J. Chem. Phys.* 46:3749–3756.

51. Logan, R. A., R. E. Coté, and P. Kusch. 1952. The sign of the quadrupole interaction energy in diatomic molecules. *Phys. Rev.* 86:280–287.

52. Flory, P. J. 1953. Principles of Polymer Chemistry. Cornell University Press, Ithaca, NY. 497–505.

53. Caines, G. H., T. Schleich, C. F. Morgan, and P. N. Farnsworth. 1990. Off-resonance rotating frame spin-lattice NMR relaxation studies of phosphorus metabolite rotational diffusion in bovine lens homogenates. *Biochemistry.* 29:7547–7557.

54. Amoore, J. E., W. Bartley, and R. van Heyningen. 1959. Distribution of sodium and potassium within the cattle lens. *Biochem. J.* 27:126–133.

55. Duncan, G., and A. R. Bushell. 1976. The bovine lens as an ion-exchanger: a comparison with ion levels in human cataractous lenses. *Exp. Eye Res.* 23:341–353.

56. Duncan, G. 1970. Movement of sodium and chloride across amphibian lens membranes. *Exp. Eye Res.* 10:117–128.

57. Lev, A. A. 1964. Determination of activity and activity coefficients of potassium and sodium ions in frog muscle fibers. *Nature (Lond.).* 201:1132–1134.

58. Reboiras, M. D., H. Pfister, and H. Pauly. 1978. Activity coefficients of salts in highly concentrated protein solutions. I. Alkali chlorides in isoionic bovine serum albumin solutions. *Biophys. Chem.* 9:37–46.